

# Development of a high stability L-band radiometer for the Aquarius ocean salinity mission

Fernando A Pellerano<sup>\*a</sup>, William J Wilson<sup>b</sup>, Alan B Tanner<sup>b</sup>

<sup>a</sup>Goddard Space Flight Center, Greenbelt, Maryland 20771 USA;

<sup>b</sup>Jet Propulsion Laboratory, California Institute of Technology, Pasadena, California 91109 USA

## ABSTRACT

The NASA Earth Science System Pathfinder (ESSP) mission Aquarius, will measure global ocean surface salinity with ~100 km spatial resolution every 7-days with an average monthly salinity accuracy of 0.2 psu (parts per thousand). This requires an L-band low-noise radiometer with the long-term calibration stability of  $\leq 0.1$  K over 7 days. A three-year research program on radiometer stability has addressed the radiometer requirements and configuration necessary to achieve this objective. The system configuration and component performance have been evaluated with radiometer test beds at both JPL and GSFC. The research has addressed several areas including component characterization as a function of temperature, system linearity, noise diode calibration, temperature control of components and optimum switching of the Dicke switch for lowest noise performance. A breadboard radiometer, utilizing microstrip-based technologies, has been built to demonstrate this long-term stability. This paper will present the results of the radiometer test program and details on the design of the Aquarius radiometer. The operational sequence that will be used to achieve the low noise and stability requirements will also be discussed.

Keywords: L-band radiometer, radiometer stability, radiometer calibration, salinity, Aquarius

## 1. INTRODUCTION

The NASA Earth Science System Pathfinder (ESSP) mission Aquarius, will measure global ocean surface salinity with ~150 km spatial resolution every 7-days with an average monthly salinity accuracy of 0.2 psu (practical salinity units or parts per thousand). Global measurements of SSS will directly aid in characterizing and understanding the current variations in global ocean circulation. The key scientific objectives of the Aquarius mission are to examine the cycling of water at the ocean's surface, the response of the ocean circulation to buoyancy forcing, and the impact of buoyancy forcing on the thermal feedback of the ocean on the climate. In addition, global surface salinity will improve our ability to model the surface solubility chemistry needed to estimate the air-sea exchange of CO<sub>2</sub>.

The Aquarius instrument, as shown in Fig. 1, will have a 2.5 m diameter offset reflector with three antenna beams operating in the pushbroom mode with a 390 km swath. Each antenna beam has a stable L-band radiometer to measure the ocean emission and determine the ocean salinity. The L-band brightness temperature variations associated with salinity changes are small, e.g. a salinity change of 0.2 psu results in a brightness temperature change of 0.1 to 0.2 K. This determines the radiometer NEDT requirement to be ~0.1 K and the stability requirement to be ~0.2 K for up to 7 days.

To develop this stable L-band radiometer, a three-year research program was undertaken under the sponsorship of the NASA Instrument Incubator Program (IIP) in 2001. This was a joint program between the Jet Propulsion Laboratory (JPL) and the Goddard Space Flight Center (GSFC). The goals of this program were to study the radiometer requirements, configuration and operational modes necessary to achieve this low noise and high stability. The system configuration and component performance have been evaluated with radiometer test beds at both JPL and GSFC. The research addressed several areas including component characterization as a function of temperature, system linearity, noise diode calibration, temperature control of components and optimum switching sequence for lowest noise performance while maintaining the required stability. This paper will present results of the radiometer test program. The

---

\* Fernando.A.Pellerano@nasa.gov; phone 1 301 286-5774; fax 1 301 286-1750

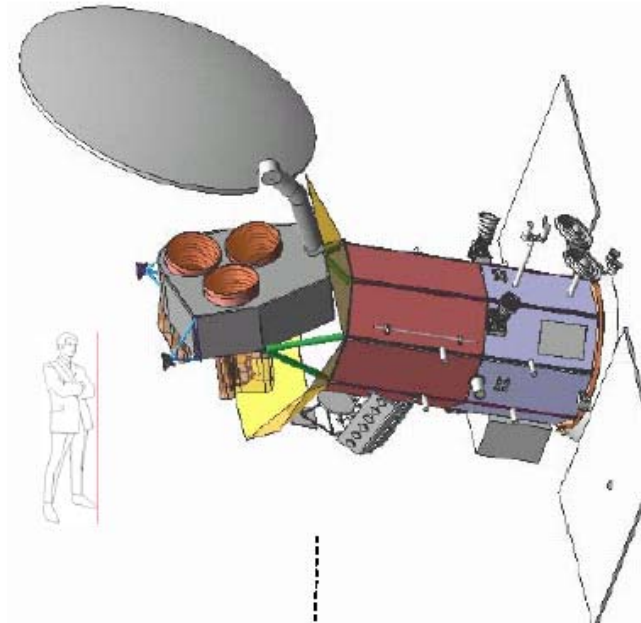


Figure 1: Aquarius ocean salinity instrument drawing. The reflector is a 2.5-m diameter offset reflector with three pushbroom antenna beams with a spatial resolution of 100-150 km.

radiometer operational sequence that will be used to achieve the low noise and stability requirements will also be discussed.

## 2. RADIOMETER TESTBEDS

At JPL, a testbed L-band radiometer was built to test out different designs necessary to achieve the low noise and high stability required for SSS measurements. A block diagram and photograph of this radiometer are shown in Fig. 2. All the radiometer components were mounted on a temperature-controlled baseplate to provide the required temperature stability.

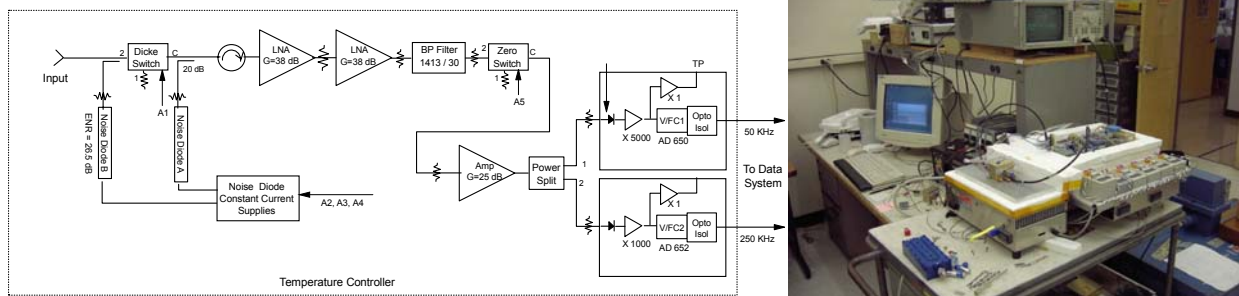


Figure 2: Block diagram and photograph of the JPL ultra stable radiometer testbed. All components were mounted on a temperature controlled baseplate and multiple noise diodes were used to cross-check the calibration stability.

At GSFC, an L-band radiometer testbed was built with the primary objective of assessing the long-term stability of the radiometers. The radiometer topology was similar to the JPL testbed, as shown in Fig. 2. This allowed us to compare results while at the same time trying complementary test scenarios. This testbed was built with a cryogenic load and operated in a thermal vacuum chamber for precise calibration control, as shown in the block diagram and picture in Fig. 3.

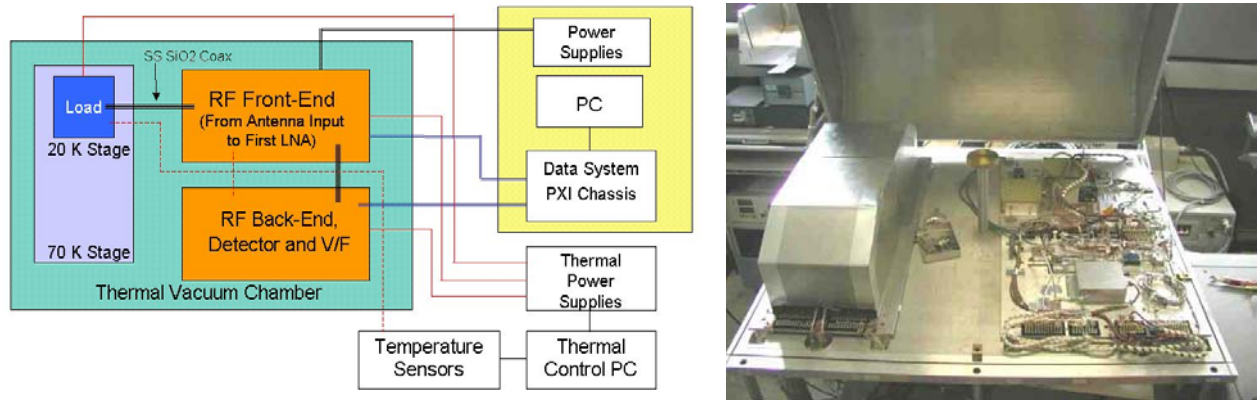


Figure 3: The testbed at GSFC provides three independently controlled temperature zones, including a cryogenic load capable of simulating ocean-like radiometric temperatures from 70K–120K.

### 3. RADIOMETER LINEARITY

A constant noise deflection method was used to measure and characterize the radiometer linearity. Using this approach, nonlinearities are observed as deviations of the noise diode deflection as the total antenna noise temperature changes. This method offers the advantage that it can be applied to the complete radiometer system, as opposed to just the final detector circuit, and because it is a ratio, it is independent of the radiometer calibration. In fact, this method can often be applied without any special accommodations or tests since the routine data from any noise-adding radiometer may be sufficient to characterize the linearity of the system as the input noise signal changes.

Fig. 4 shows the laboratory configuration of the linearity deflection test. The antenna in this case was replaced with a cold source and an injected noise source, which could be adjusted between ~30 K and 4700 K, well below and above the expected operational range. Also, the noise diode was injected after the Dicke switch so that the deflection can be measured in both the ‘antenna’ and ‘reference’ modes of the switch. With both of these measurements the antenna deflections can be normalized and the linearity examined with the deflection ratio:

$$D = \frac{V_{AN} - V_A}{V_{ON} - V_O}, \tag{1}$$

where the four voltages represent the response to the antenna ( $V_A$ ), antenna plus noise diode ( $V_{AN}$ ), ambient temperature reference ( $V_O$ ), and reference plus noise diode ( $V_{ON}$ ). In a linear system with no impedance mismatches,  $D$  should always be unity. If the system is nonlinear, then  $D$  will change as the antenna noise temperature changes.

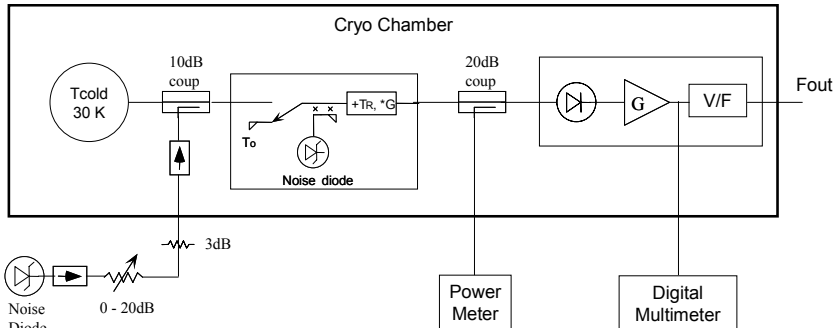


Figure 4: This setup for linearity tests using the deflection method allows the radiometer input to vary from 30 K – 4700 K without changing any radiometer circuitry.

As shown by the red '+' in Fig. 5, the system has a gain expansion behavior, as expected from the detectors, at low power levels up to approximately 2 mW, and gain compression at the higher levels. The response can be linearized very successfully with an error < 0.04% using a third order polynomial fit, as shown by the blue 'x'. These results also showed a bias in the deflection ratio due to the impedance mismatch of the Dicke switch between the antenna and load ports. This effect arises due to the coupler's imperfect isolation. Placing an isolator between the Dicke switch and the coupler eliminated this problem.

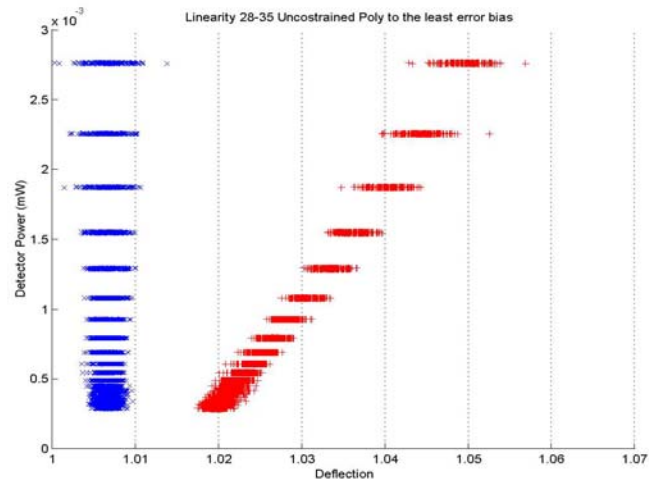


Figure 5: The radiometer can be linearized very successfully with a 3rd order polynomial.

Tests were also performed to assess the linearity as a function of temperature. Two different scenarios were used. In the first one the radiometer front- and back-ends were held at equal temperatures in five temperature steps, 280 K, 289 K, 290 K, 291 K, and 300 K. The second scenario held the temperature of the front-end at a constant 290 K while the back-end was stepped through the above temperatures. In each of these tests the radiometer was allowed to settle and temperature-stabilize. The results show that for either of these cases the change in linearity as a function of temperature is very small. With a radiometer gain of approximately 0.1 K/Hz, the variation of the linearity is on the order of 0.04 K/°C in the expected ocean temperature range, and 0.15 K/°C in the noise diode injected temperature range. These effects become negligible given that the radiometer physical temperature will be stable to < 0.1°C RMS. Similar results were obtained for the second scenario of split temperatures. It is actually remarkable that we can detect these very small variations with this radiometer with the deflection technique.

#### 4. RADIOMETER NOISE MODEL AND OPTIMUM OPERATING SEQUENCE

A model for the Aquarius microwave radiometer is described below with the equations that will be used to calibrate the radiometer data. With Aquarius, it is planned to use a switching sequence, using the running averages of gain and radiometer noise, to minimize the RMS noise and maintain the required stability. This switching sequence is based on the measured properties of the radiometer; i.e., the power spectra of the gain and radiometer noise, and has been analyzed and demonstrated during the IIP research on the ultra stable radiometer.

To accurately calibrate a microwave radiometer, it is necessary to know the loss and temperature of every front-end component to calculate its emission temperature, and to measure the gain and radiometer noise temperature to calibrate the output signal to the input noise temperature. A model of the Aquarius radiometer is shown in Fig. 6. To simplify this discussion, this model will be defined to have only three temperature zones. (In practice, it will probably be necessary to use additional temperature zones to accurately represent the separate components.)

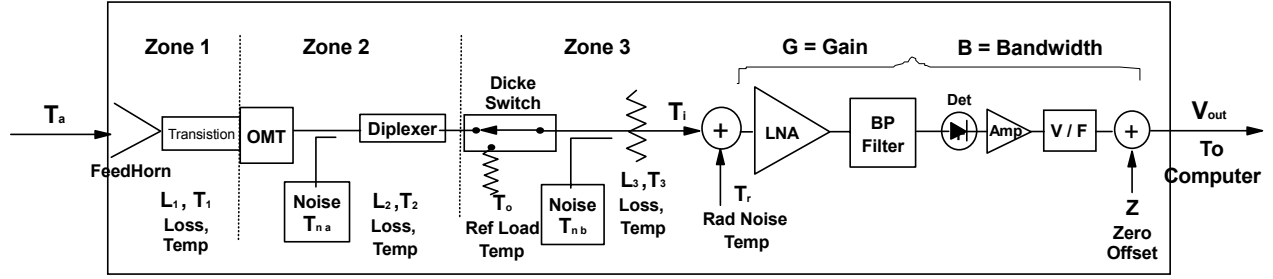


Figure 6: Aquarius Radiometer Model

The input temperature to the low noise amplifier (LNA),  $T_i$ , is given by the following radiative transfer equation,

$$T_i = \frac{T_a}{L_1 * L_2 * L_3} + \frac{T_1}{L_2 * L_3} \left[ 1 - \frac{1}{L_1} \right] + \frac{T_2}{L_3} \left[ 1 - \frac{1}{L_2} \right] + T_3 \left[ 1 - \frac{1}{L_3} \right] \quad (2)$$

where  $L_1, L_2, L_3$  = Ohmic losses in Zones 1, 2, and 3,  
 $T_1, T_2, T_3$  = physical temperatures of losses  $L_1, L_2, L_3$  (K),  
 $T_a$  = antenna temperature (K).

This equation can be solved for the desired antenna temperature,  $T_a$ :

$$T_a = L_1 * L_2 * L_3 * T_i - T_1 * (L_1 - 1) - L_1 * T_2 * (L_2 - 1) - L_1 * L_2 * T_3 * (L_3 - 1) \quad (3)$$

A radiometer operational technique that provides lower noise performance than either the two- or three-position Dicke switching technique is a method that observes the input signal most of the time and only uses a small amount of the time to measure the gain  $G$ , the radiometer noise temperature  $T_r$ , and the zero offset  $Z$ . In this calibration technique, running averages of  $G$  and  $T_r$  are used to reduce the errors in these estimates. Using the running average estimates of these two parameters, the input temperature,  $T_i$ , is given by the expression:

$$\hat{T}_i = \frac{V_i}{\langle G \rangle} - \langle T_r \rangle, \quad (4)$$

where  $V_i$  = output voltage when observing the antenna  
 $\langle G \rangle$  = running average of the gain  
 $\langle T_r \rangle$  = running average of the radiometer noise

The length of the running averages is set by the stability of  $G$  and  $T_r$  measurements, which can be determined by measuring their power spectra and noting at what frequency their  $1/f$  noise becomes dominant. This  $1/f$  point is a function of the switching sequence used and the temperature stability of the radiometer components. In our laboratory radiometer system, which had 60% of the time spent on the input and was temperature controlled to  $\pm 0.1^\circ\text{C}$ , the  $1/f$  point of  $G$  was  $>150$  seconds. The radiometer noise temperature,  $T_r$  is a more stable quantity and its  $1/f$  point had values  $> 3,000$  seconds. (Note that these values are stated as the inverse frequency to provide a better physical understanding.) Using these long-running averages in the measurements of  $G$  and  $T_r$  then reduces the RMS noise in the measured input temperature,  $\Delta T_i$ , while still achieving the long-term stability.

A calculation of  $\Delta T_i$  versus the input temperature  $T_i$  shows that using the running averages of  $G$  and  $T_r$  to continuously calibrate the radiometer, the  $\Delta T_i$  is only increased by a factor of  $\sim 1.5$  compared to an “ideal” total power radiometer. This technique has a  $\Delta T \sim 1.6$  times lower than the standard two-position Dicke-switched radiometer and  $\sim 2$  times lower than the three-position Dicke-switched radiometer.

### 5. RADIOMETER STABILITY TESTS

In November and December 2004, long-term stability tests each of 5 to 8 days’ length were made with the JPL laboratory testbed radiometer. Two calibration sources were used: a temperature controlled hot load with an effective temperature of  $\sim 366$  K, and a temperature-controlled LNA, which was the cold load with an effective temperature of  $\sim 64$  K. Both the hot and cold loads were used with the testbed radiometer in two temperature environments. The first was a  $\pm 0.1^\circ\text{C}$  temperature controlled environment and the second was the ambient laboratory environment where the radiometer temperature variations were typically  $\pm 0.5^\circ\text{C}$ .

Results from the hot load during the  $\pm 0.1^\circ\text{C}$  tests for 7.6 days are shown in Fig. 7. Plots of the power spectra of the gain,  $T_r$ , and  $T_a$  versus  $1/f$  are shown in Fig. 8. The  $1/f$  point where the power starts to increase is also noted in the figure. Note that at the longer time scales (lower frequencies), the increase in gain and  $T_r$  is proportional to  $1/f$ . (The increase in these power spectra at  $\sim 500$  seconds is due to the switching of the  $\pm 0.1^\circ\text{C}$  temperature controller.) The physical temperatures of the baseplate and input coax, the averaged gain and  $T_r$ , and the radiometer antenna temperature,  $T_a$ , are also shown in Fig. 7. Both the gain and baseplate temperature reflect the switching of the temperature controller. The RMS of the radiometer antenna temperature over the entire 8-day period is 0.10 K for the 5-sec samples. The model calculations predicted that the RMS should be 0.08 K. This slightly larger measured value may be due to instability in the hot-load temperature controller and the small error in the correction that was used for the input coaxial line. The other results from the stability tests using the “cold” load were also consistent with the model predictions.

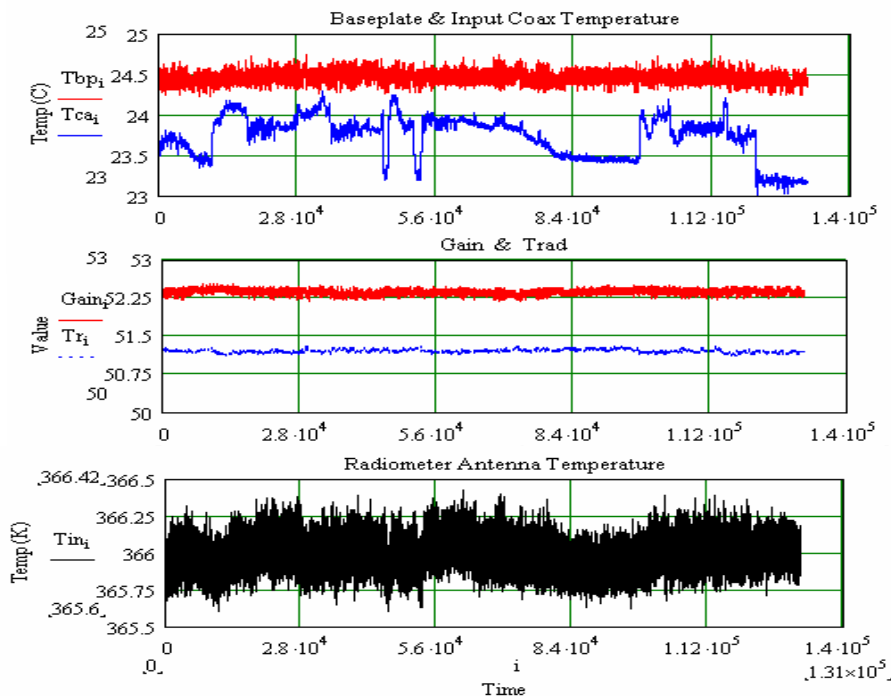


Figure 7: 5-second sample data from the 7.6-day test with the hot load with  $\pm 0.1^\circ\text{C}$  radiometer temperature control. The RMS of the baseplate temperature (top red) was  $0.08^\circ\text{C}$ . The gain average (lower red) is 75 seconds and was offset by 30. The  $T_r$  average was 1275 seconds. The RMS of the radiometer antenna temperature is 0.10 K over the full 7.6 days.

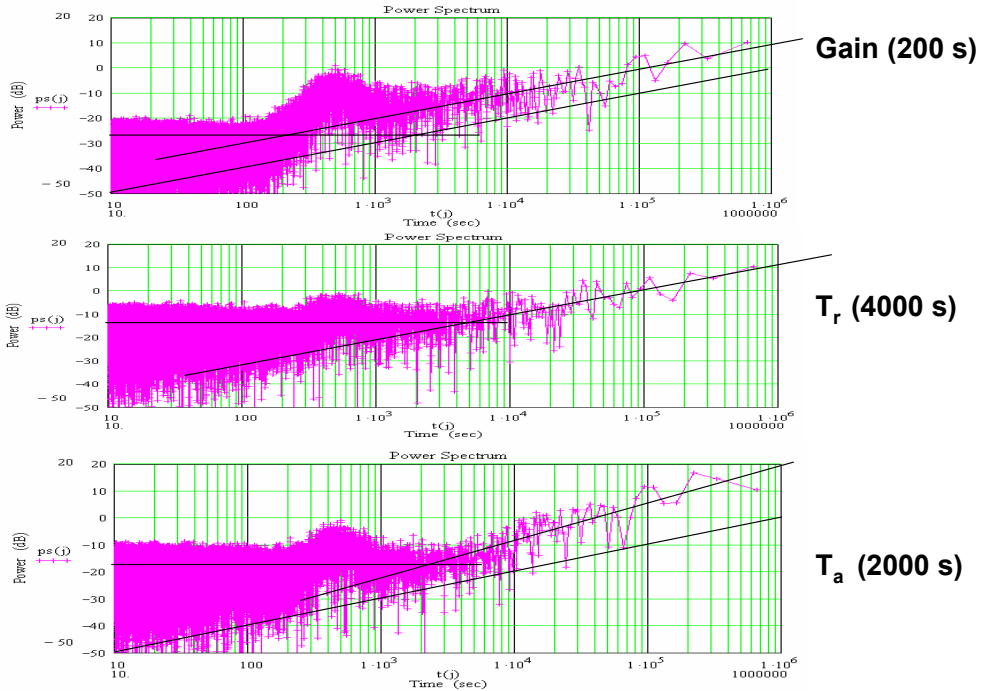


Figure 8: Power spectra for the Gain,  $T_r$ , and  $T_a$  plotted versus  $1/f$  (sec) for the hot load with  $\pm 0.1^\circ\text{C}$  radiometer temperature control for 7.6 days. The “ $1/f$ ” points where the power increases for lower frequencies are noted on the right. The black lines through the low frequency values are proportional to  $1/f$ , except for  $T_a$ , which increases slightly faster.

## 6. SUMMARY

This ultra stable radiometer research project addressed the problem of how to design and build a low-noise microwave radiometer to achieve the calibration stability of  $<0.1$  K over 7 days as required for the Aquarius salinity instrument. The key result has been that precise temperature control of all the radiometer components is required to meet this requirement. This result was then demonstrated with the testbed radiometers. In addition, we have demonstrated that with a stable temperature environment, using long-term running averages of the radiometer gain ( $G$ ) and the noise temperature ( $T_r$ ) results in the lowest noise performance with the required stability. An analytical noise model to optimize the switching sequence for the lowest noise, based on the power spectra of the gain and  $T_r$ , was also developed. Other stability issues that were addressed in this research were a procedure for measurement and correction for radiometer system non-linearity and temperature control requirements to achieve the required stability. The practical result of this research was the incorporation of these results into the design of the Aquarius radiometers.

There is the question as to what limits the long-term calibration stability of the radiometer. The answer is that the long-term calibration depends on the stability of all the front-end components. Most of these components are passive, and if their temperature is controlled, they are expected to be stable. The two active components, which may change over weeks to month time periods, are the noise diode output power and the PIN diode Dicke switch loss. Based on our experience with the spaceborne noise diodes and PIN diode switches in the Topex/Poseidon and Jason missions, these changes are very small and only detectable after months of time. In the Aquarius mission, it is planned to observe stable Earth-based targets, e.g., the Dome-C in Antarctica and large numbers of ocean buoys, to monitor and then correct for any long-term drifts. Given that everything that we know how to do to build a stable radiometer is being done, the Aquarius mission will provide an excellent example of a stable microwave radiometer.

## ACKNOWLEDGMENTS

This study was sponsored by the Instrument Incubator Program (IIP) of the NASA Earth-Sun System Technology Office (ESTO). The authors thank George Komar, Ken Anderson, and Tom Cwik of the ESTO Program Office for their support and guidance of the study. The authors also thank their colleagues in the Aquarius Project. In particular Gary Lagerloef, Principal Investigator from Earth and Space Research, and David LeVine, Co-Principal Investigator from NASA-GSFC for all their help and useful discussions on this subject. Part of the research described in this paper was carried out at the Jet Propulsion Laboratory, California Institute of Technology, under a contract with the National Aeronautics and Space Administration.

## REFERENCES

1. William Wilson, Alan Tanner, Fernando Pellerano, and Kevin Horgan, *Ultra Stable Microwave Radiometers for Future Sea Surface Salinity Missions*, JPL Report D-31794, April 2005.